Performance Verification of an Adaptive 100% Injection-Based Stator Ground Fault Protection Using a Large MVA Generator

Nader Safari-Shad, *Senior Member, IEEE*, Russ Franklin

***Abstract*—The paper reports on performance verification of a newly developed adaptive injection-based 100% stator ground fault protection scheme. The verification is achieved by measuring the neutral grounding signals of an existing conventional subharmonic injection relay used for protection of a 618 MVA synchronous generator. The process of signal measurements, signal conditioning, and setting up alarm and trip equations is explained in detail. The results not only confirm the expected performance reported earlier on a 5 kVA lab generator, but also prove the applicability of the new adaptive scheme to stator ground fault protection of large MVA generators under typical industrial conditions.**

***Index Terms*—Synchronous generator stator ground fault protection, 100% subharmonic injection method, Kalman adaptive filtering, Stator ground fault location.**

I. Introduction

The fault-free operation of large synchronous generators in power systems is of paramount importance. Despite best maintainance practices, however, generator faults do happen resulting in downtimes and high repair costs. Perhaps, the most common fault in synchronous generators is the stator windings ground fault which can be catastrophic when protective relays fail to protect 100% of the stator windings [1].

Most stator windings ground fault protective schemes must be used in conjunction with one another to provide 100% ground fault protection [2]. A stator ground fault protection which is applicable to high-impedance grounded (HIG) synchronous generators is the subharmonic injection scheme known as the 64S [3]. Early implementation of this scheme appeared as a subharmonic overcurrent scheme believed to provide 100% stator windings ground fault protection single-handedly [4]. However, this type of 64S scheme was later shown to be insensitive to high-impedance ground faults particularly in case of generators which have a large total capacitance to ground [5] - [8].

The concern about dependability of the overcurrent-based 64S scheme has led to several commercially available impedance-based 64S protective relays [9] - [13]. The operational theory of these relays is reviewed in [14] and is based on real-time stator insulation resistance estimation where it is assumed that all circuit parameters are measurable during field commissioning. Among these parameters are the input resistance of the subharmonic injection source, the impedance of its associated bandpass filter, the neutral grounding resistance and the total generator capacitance. Since the actual value of these parameters varies with temperature, time, deformation of the stator windings and system voltage, the non-adaptive insulation resistance estimation methods may be inaccurate. For this reason, the use of Kalman adaptive filtering (KAF) has been suggested in [14] for real-time stator winding insulation parameter estimation. In this adaptive 64S scheme, called *A64S scheme*, the stator time constant and insulation resistance are identified in real-time without the need for any parameter measurements during field commissioning.

Although [14] verified the performance of the A64S scheme by conducting extensive fault-free and faulty experiments, this verification was obtained using a 5 kVA lab generator under some restrictive conditions. Specifically, small scale of the lab generator and limitation of sensing low level subharmonic current signals required adding large compensation capacitances without the need for a normally available current transformer (CT) in the neutral grounding circuit. These deviations from real-world applications have naturally led to a desire for obtaining a performance verification using a large MVA generator. The present paper aims to fulfill exactly this goal. Specifically, a 618 MVA unit-connected generator in Alliant-Energy generation fleet is selected for performance verification purposes. This unit has an installed overcurrent-based 64S relay [15] which although captures the required subharmonic signals, it does not provide them to the user in a usable form. Hence, measuring the required subharmonic signals is conducted independently during a recent scheduled maintainance outage of the unit. The paper presents the complete process of signal measurements and analysis leading to performance evaluation of the A64S scheme during fault-free and faulty modes. The results not only confirm the expected performance reported earlier on the 5 kVA lab generator, but also prove the applicability of the new adaptive scheme to stator ground fault protection of large MVA generators under typical industrial conditions.

II. Operational Theory of the A64S Scheme

In this section, we briefly summarize the operational theory of the A64S scheme. The reader is referred to [14] for more details.

Fig. 1 depicts the schematics of a neutral grounding circuit in HIG generators equipped with a A64S relay.

N. Safari-Shad is with the Department of Electrical and Computer Engineering, University of Wisconsin-Platteville, 1 University Plaza, Platteville, WI 53818 USA (e-mail: safarisn@uwplatt.edu).

R. Franklin is with the Alliant Energy Corporate Services, Inc., 4902 N. Biltmore Lane, Madison, WI 53718 USA (e-mail: russfranklin@alliantenergy.com).

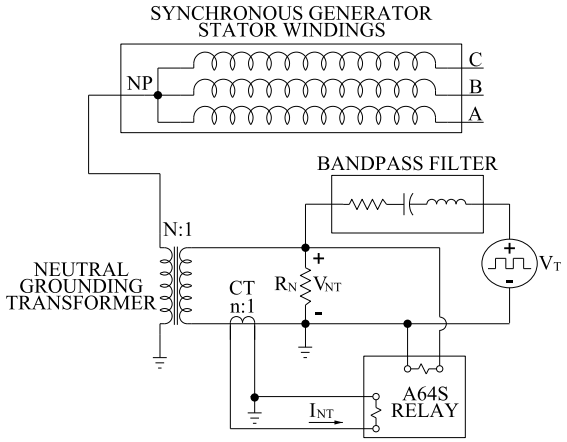

Fig. 1. Implementation of the A64S scheme in HIG generators

In this circuit, the subharmonic voltage source V_T is typically a square-wave signal with frequency of $15-20$ Hz and an rms value of 26 V under load. When V_T is powered on, the bandpass filter (BPF) ensures that the voltage across neutral grounding resistor R_N is sinusoidal at the subharmonic frequency. This causes a current flow through the generator stator windings and the capacitance to ground of the generator, its iso-phase bus work and delta-windings of its step-up transformer.

Fig. 2 depicts the equivalent circuit model of the neutral grounding subharmonic injection circuit where R_S and C_0 represent the unfaulted stator insulation resistance, and total generator capacitance seen by the subharmonic injection source, respectively.

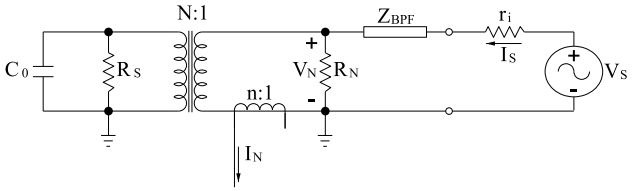

Fig. 2. Equivalent circuit model of the neutral grounding subharmonic injection circuit

Reflecting the total generator capacitance C_0 and the stator insulation resistance R_S onto the secondary side of the neutral grounding transformer, the simplified equivalent circuit model is shown in Fig.3.

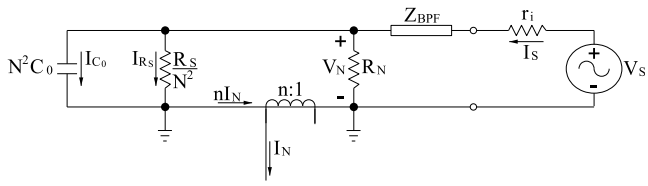

Fig. 3. Simplified equivalent circuit model of a HIG subharmonic injection system

Based on this circuit model, the relationship between the subharmonic neutral signals V_N and I_N is governed by a first-order differential equation given by

$$\tau_0 \, \frac{dV_N(t)}{dt} + V_N(t) = K_c \, I_N(t) \tag{1}$$

where $\tau_0 = R_S \, C_0$ is the stator time constant and $K_c = \frac{n \, R_S}{N^2}$. This model can be discretized using the trapezoidal numerical integration rule [16] to yield a first-order difference equation

$$V_{N,k} + a_0 \, V_{N,k-1} = K_d \, (I_{N,k-1} + I_{N,k}) \tag{2}$$

suitable for the discrete-time application of KAF parameter estimation. Note that in (2),

$$a_0 = \frac{T - 2\,\tau_0}{T + 2\,\tau_0}, \qquad K_d = \frac{K_c \, T}{T + 2\,\tau_0} \tag{3}$$

where k is the kth sampling instance and $T > 0$ is the sampling period. Note that the discrete-time model parameters a_0 and K_d are uniquely represented by the original continuous-time model parameters R_S and τ_0.

Given V_N and I_N sample values, the KAF algorithm estimates the parameters a_0 and K_d according to [17]:

$$\begin{aligned}
&\hat{\theta}_k = \hat{\theta}_{k-1} + G_k \, \nu_k \,, && \hat{\theta}_0 = \bar{\theta}_0 \\
&\nu_k = V_{N,k} - \phi_k^T \, \hat{\theta}_{k-1} \\
&G_k = \frac{1}{\sigma_w^2} \, P_k \, \phi_k \\
&P_k = \frac{P_{k-1} \, \sigma_w^2}{\sigma_w^2 + \phi_k^T \, P_{k-1} \, \phi_k} + \sigma_v^2 \, \mathrm{I}_2 \,, && P_0 = \bar{P}_0
\end{aligned} \tag{4}$$

where a_0 and K_d are described by the stochastic parametric model

$$\begin{aligned}
\theta_{k+1} &= \theta_k + v_k \,, \qquad i.c. = \theta_0 \\
V_{N,k} &= \phi_k^T \, \theta_k + w_k
\end{aligned} \tag{5}$$

with

$$\theta_k = \begin{bmatrix} a_{0,k} \\ \\ K_{d,k} \end{bmatrix}, \quad \phi_k^T = \begin{bmatrix} -V_{N,k-1} & I_{N,k-1} + I_{N,k} \end{bmatrix} \tag{6}$$

Here, it is assumed that the *initial condition* θ_0 is a Gaussian random parameter vector with mean $\bar{\theta}_0$ and covariance $\bar{P}_0$. Moreover, v_k and w_k are zero-mean white noise processes with covariances

$$E\{v_i \, v_j^T\} = \sigma_v^2 \, \mathrm{I}_2 \, \delta_{ij}, \quad E\{w_i \, w_j\} = \sigma_w^2 \, \delta_{ij}$$

where E is the expectation operator and θ_0, v_k and w_k are mutually uncorrelated.

Once the parameter vector θ_k is estimated by

$$\hat{\theta}_k = \begin{bmatrix} \hat{a}_{0,k} & \hat{K}_{d,k} \end{bmatrix}^T$$

the original continuous-time model parameter estimates can be extracted, i.e.,

$$\hat{\tau}_0(t) = \frac{T}{2} \, \Psi \left(\frac{1 - \Phi(\hat{a}_{0,k})}{1 + \Phi(\hat{a}_{0,k})} \right) \tag{7}$$

$$\hat{R}_S(t) = \frac{N^2}{n \, T} \, \Psi \left((T + 2\,\hat{\tau}_0(t)) \, \Phi(\hat{K}_{d,k}) \right) \tag{8}$$

Here, $\Phi(\cdot)$ is a *smoothing operator* consisting of a zero-order hold operation followed by a first-order low-pass analog filter given by

$$F(s) = \frac{\gamma}{s+\gamma}\,, \qquad \gamma > 0 \tag{9}$$

Moreover, $\Psi(\cdot)$ is an *activation operator* defined by

$$\Psi(q) = \begin{cases} q\,, & \text{if } q \geq 0 \\ 0\,, & \text{otherwise} \end{cases}$$

Note that the operator Φ is used for converting from discrete-time to continuous-time as well as signal conditioning while Ψ is used to reject any negative parameter estimates generated during transient periods.

Using the estimated stator resistance $\hat{R}_S(t)$, *under-resistance* alarm and trip equations can be specified to detect stator ground faults, i.e.,

$$\begin{aligned} \textbf{Alarm if}: &\quad \hat{R}_S(t) < \beta_1 \\ \textbf{Trip if}: &\quad \hat{R}_S(t) < \beta_2 \end{aligned} \tag{10}$$

where β_1 and β_2 are the respective alarm and trip pickup settings. The procedure for selecting suitable values for β_1 and β_2 will be presented in Section IV.

Note that while tracking sudden changes in $\hat{R}_S$ can lead to stator solid ground fault detection as outlined above, tracking subtle changes in $\hat{\tau}_0$ can lead to a *dissipation factor* (DF) [18] monitoring capability which is an indicator of dielectric losses in all three phases and general stator condition [19]. To see this latter capability, consider the simplified equivalent circuit in Fig. 3. According to [18], DF is defined by the magnitude of the ratio of I_{R_S} to I_{C_0} which is readily shown to be equal to

$$DF = \frac{1}{\omega_0\, \tau_0} \tag{11}$$

with ω_0 as the angular subharmonic frequency. Hence, the A64S scheme can also provide an overall (average) estimated DF monitoring capability in real-time.

III. Generator Subharmonic Signal Measurements

The HIG synchronous generator selected for the performance verification of the A64S scheme is shown in Fig. 4.

Fig. 4. 618 MVA unit selected for performance verification of the A64S scheme

This unit is protected by two multi-function microprocessor relays one of which has a conventional overcurrent-based 64S scheme. However, as mentioned earlier, the required subharmonic signals for the A64S performance verification cannot be obtained from this relay. Hence, these signals are measured using two current probes, one voltage probe, and a digital storage oscilloscope. The reason two current probes are used is to measure the total neutral current I_{NT} on the secondary as well as the primary side of neutral grounding CT. In this way, the CT performance which is used for the conventional overcurrent-based 64S application can be evaluated.

To carry out the verification, it is decided to measure the required signals under one fault-free and two faulty modes, i.e.,

Case i): no ground fault on the stator;
Case ii): stator grounded at the neutral;
Case iii): stator grounded at the terminal on phase A.

Once the injection source is turned on, all signal measurements are conducted on the low-side of the neutral grounding transformer circuit shown in Fig. 5.

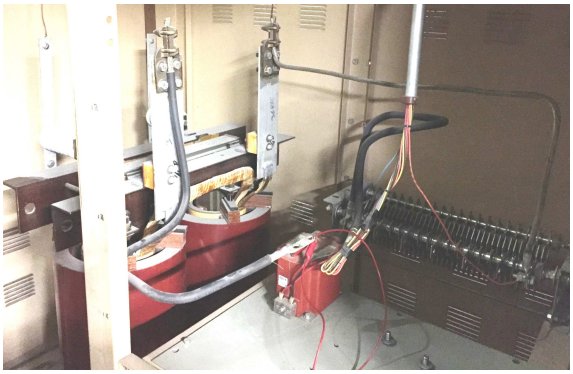

Fig. 5. Typical neutral grounding circuit of HIG generators

Table I lists the specifications of all equipment in the neutral grounding circuit as well as signal measuring devices used. In all measurements, the oscilloscope records 5 seconds of all three signals simultaneously at 0.1 msec sampling rate.

TABLE I
SPECIFICATIONS OF THE NEUTRAL GROUNDING CIRCUIT EQUIPMENT AND SIGNAL MEASURING DEVICES

Equipment	**Description**
Grounding Transformer	Rated at 75 kVA with 60 : 1 ratio
Neutral grounding CT	Relaying class T50 with 400 : 5 ratio
Subharmonic source	Siemens 7XT33 (20 Hz)
Bandpass filter	Siemens BPF 7XT34
Digital storage oscilloscope	LeCroy Wavesurfer 3024
Two current sensors	LeCroy CP030 probes
Voltage sensor	LeCroy PP019 probe
Neutral grounding resistor	$R_N = 0.35\,\Omega$

IV. Analysis of Measured Signals

In this section, the fault-free measured signals are first analyzed. Based on this analysis and the use of KAF estimator,

the fault-free insulation resistance of the generator is estimated. Moreover, reasonable alarm and pickup setting criteria for implementation of the A64S fault detection scheme are suggested. Finally, the neutral and terminal faulty measured signals are used to obtain the fault response of the A64S scheme.

A. *Fault-free Case:*

Fig. 6 shows the case i) signal captures where for the sake of clarity, only a 2 second segment of the recorded signals is displayed.

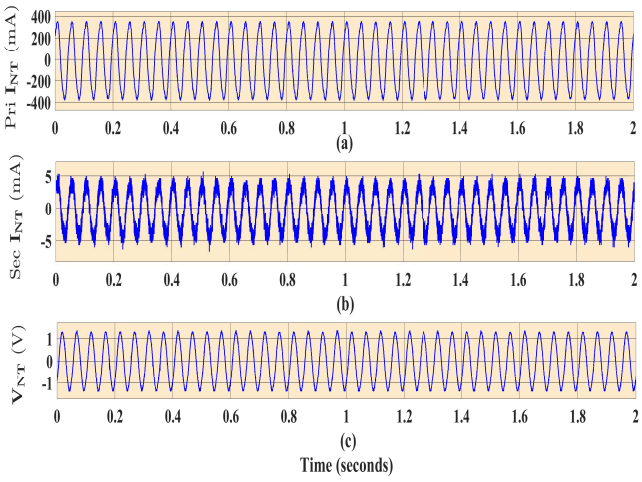

Fig. 6. Case i) signals: (a) Primary total neutral current I_{NT}, (b) secondary total neutral current I_{NT}, (c) total neutral voltage V_{NT}

From plot (b) in Fig. 6, it is evident that there is considerable noise in the secondary total neutral current signal I_{NT}. To remove the noise, all signals are filtered using a 20-Hz bandpass filter with transfer function

$$H_{20}(s) = \left(\frac{12.63\, s}{s^2 + 12.63\, s + 1.579 \times 10^4} \right)^2 \qquad (12)$$

Fig. 7 shows the filtered signals which are renamed as (a) primary filtered neutral current I'_N, (b) secondary filtered neutral current I_N, and (c) filtered neutral voltage V_N.

To investigate the effect of the neutral grounding CT on the recorded measurements, the primary and secondary neutral current signals are plotted on the same axis. Plot (a) in Fig. 8 shows the primary neutral current I'_N normalized by the nominal CT ratio of 80 and the secondary neutral current I_N. Close inspection of the time difference between the two signals reveals that an approximately 1.7 msec time-delay is introduced by the CT. Moreover, the amplitudes are different which implies the effective CT ratio is slightly different from the nominal value. Similarly, plot (b) in Fig. 8 shows that I_N leads V_N by about 94 electrical degrees. This amount of phase difference violates the subharmonic injection circuit model described by (1). Hence, a calibration on both magnitude and phase of I_N must be performed to compensate for CT nonideality. It turns out that all commercial impedance-based 64S relays perform similar types of calibrations to ensure

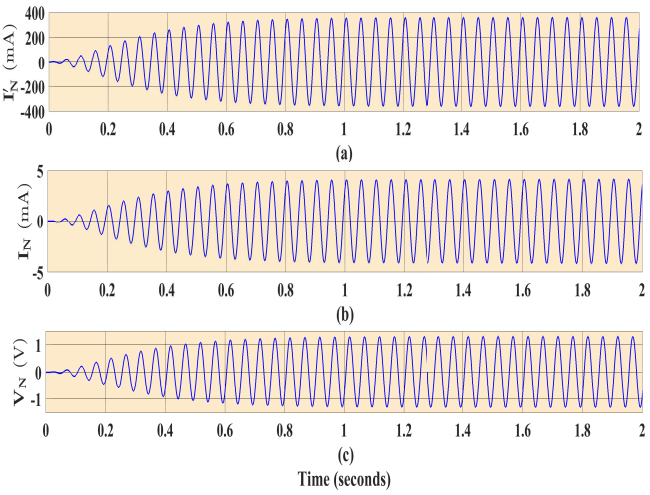

Fig. 7. Case i) 20 Hz bandpass filtered signals: (a) Primary neutral current I'_N, (b) secondary neutral current I_N, (c) neutral voltage V_N

model assumptions are satisfied, see e.g., [20] and [21]. In our case, the calibration process is conducted simply by time-delaying I_N by 1.7 msec (17 sampling periods) and using an effective CT ratio of $n_e = 87$.

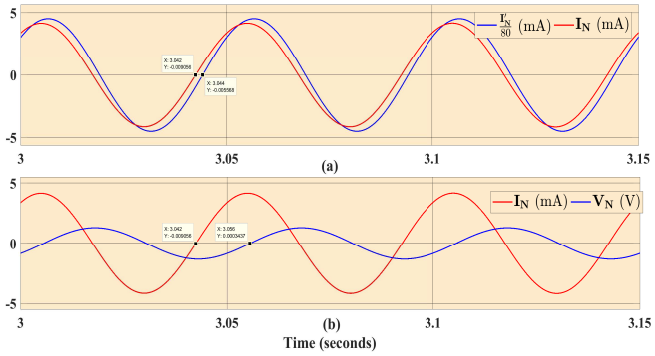

Fig. 8. Case i) zoomed in filtered signals: (a) normalized I'_N and I_N, (b) I_N and V_N

To obtain the stator insulation parameter estimates, the captured signals are fed into a Matlab/Simulink code which performs the required bandpass filtering and signal calibration, KAF estimation as well as the mappings Φ and Ψ according to the block diagram shown in Fig. 9.

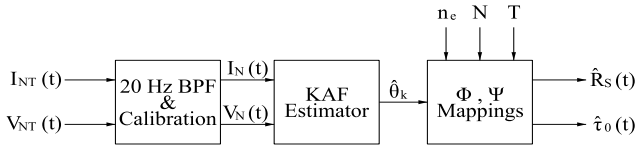

Fig. 9. Block diagram of the adaptive injection-based stator insulation parameter estimates

Table II displays the settings used by the block diagram depicted in Fig. 9. Note that the settings $\bar{\theta}_0$, $\bar{P}_0$, σ_v^2, σ_w^2, and γ used in the KAF estimator block and Φ mapping are the same as those used in [14] for the 5 kVA lab generator.

This observation is important since it shows that the required KAF parameter estimation settings are not generator specific. In contrast to these, the settings n_e and N are specific to the equipment used in the neutral grounding circuit of the 618 MVA generator. Finally, the sampling period T is a user selected setting which depends on the capability of the particular data acquisition system used. In our case, since the subharmonic injection source uses a 20 Hz signal frequency, a sampling period of 0.1 msec is quite sufficient.

TABLE II
KAF PARAMETER ESTIMATION SETTINGS

$\bar{\theta}_0$	$\bar{P}_0$	σ_v^2	σ_w^2	γ	n_e	N	T
$0_{2\times1}$	10 I_2	5	0.01	50	87	60	0.1 msec

Using Table II values, Fig. 10 shows the fault-free stator insulation parameter estimates using the full range of signal captures.

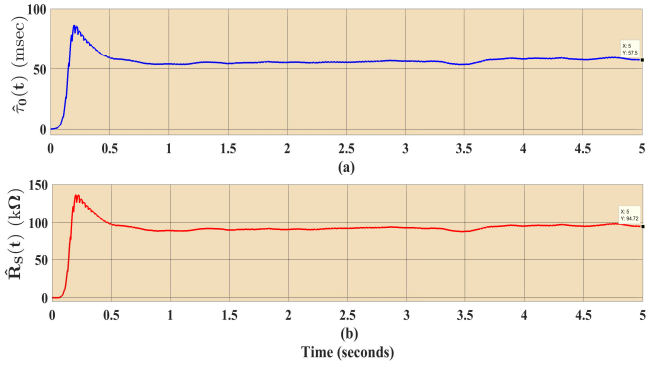

Fig. 10. (a) Fault-free stator insulation time constant estimate and (b) fault-free stator insulation resistance estimate

From plots (a) and (b), it can be seen that both unfaulted insulation parameters are estimated (learned) quickly despite starting at zero initial conditions. In particular, we note that $\hat{R}_S = 94.72$ kΩ at $t = 5.0$ sec.[1] Based on this value, under-resistance alarm/trip pickup settings for the 618 MVA generator are calculated at 50% and 10% of 94.72 kΩ, respectively. These choices yield the following alarm/trip equations

$$\begin{aligned} \textbf{Alarm if}: &\quad \hat{R}_S(t) < 47.5\ k\Omega \\ \textbf{Trip if}: &\quad \hat{R}_S(t) < 9.5\ k\Omega \end{aligned} \tag{13}$$

Note that while the alarm pickup criterion is selected arbitrarily, the trip pickup criterion follows the 90% insulation breakdown criterion suggested in [22].

[1]It must be pointed out that although the unfaulted stator insulation resistance measured by offline megger testing methods is usually higher, given the input power of the subharmonic injection source, this estimated value is typical of the fault-free insulation resistance estimated by conventional impedance-based 64S relays, see e.g. [21]

B. *Staged Neutral Ground Fault Case:*

A neutral ground fault scenario is staged in this case by installing a short circuit between the generator neutral and the ground using twelve feet of 4 AWG copper wire which has a resistance R_{Sf} of approximately 3.0 mΩ. The schematics of the neutral grounding circuit for this case is shown in Fig. 11 where the total generator capacitance C_0 is shown as equally distributed among the terminal phases.

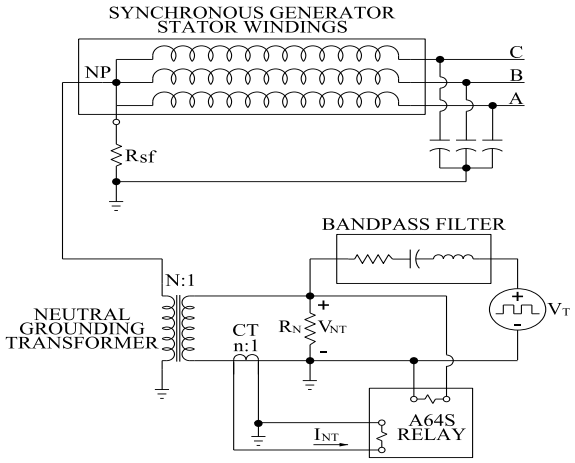

Fig. 11. Schematic of the neutral grounding circuit with an installed short at the generator neutral

Fig. 12 shows the case ii) signal captures, i.e., secondary total neutral current I_{NT}, secondary calibrated 20 Hz neutral current I_N, total neutral voltage V_{NT}, and its 20 Hz component V_N. Note that for clarity, only 1 second of the unfaulted

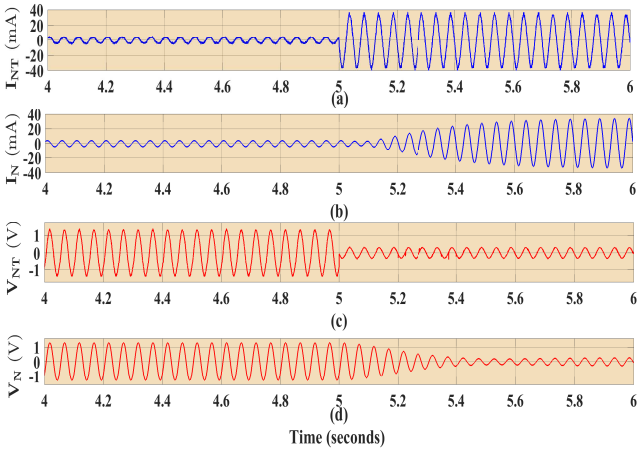

Fig. 12. Case ii) zoomed in signals: (a) Total secondary neutral current I_{NT}, (b) calibrated 20 Hz secondary neutral current I_N, (c) total neutral voltage V_{NT}, and (d) 20 Hz neutral voltage V_N

signals followed by 1 second of neutral ground fault signals are shown.

Fig. 13 shows the corresponding stator insulation parameter estimates before and after the staged neutral ground fault. It is clear that using the A64S scheme with the trip equation as defined by (13), this fault would be quickly detected after a short transient.

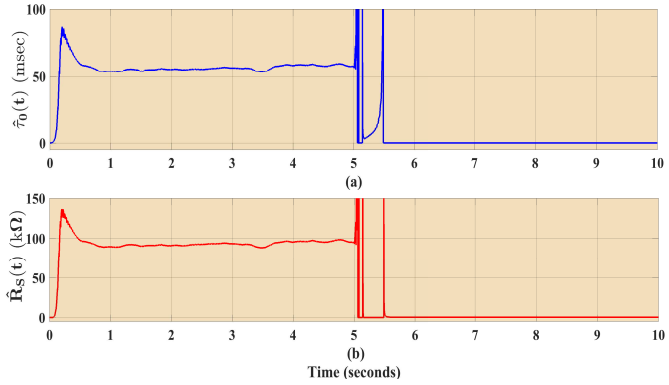

Fig. 13. Case ii): (a) Stator insulation time constant, and (b) stator insulation resistance

C. Staged Terminal Ground Fault Case:

In this case, a terminal ground fault scenario is staged by installing a short circuit between the generator terminal phase A and the ground using the same copper wire as in Case ii). The schematics of the neutral grounding circuit for this case is shown in Fig. 14.

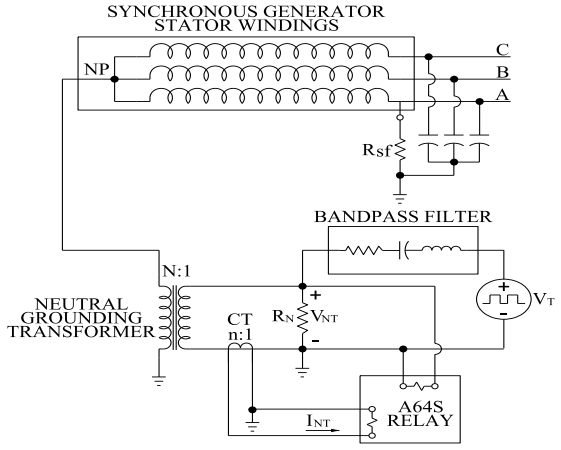

Fig. 14. Schematic of the neutral grounding circuit with an installed short at the generator terminal phase A

Fig. 15 shows the case iii) signal captures, i.e., secondary total neutral current I_{NT}, its calibrated 20 Hz component of I_{NT}, total neutral voltage V_{NT}, and its 20 Hz component.

Fig. 16 shows the corresponding stator insulation parameter estimates before and after the staged ground fault at the terminal phase A. Once again, it is clear that using the A64S scheme with the trip equation as defined by (13), this fault would be quickly detected after a short transient.

V. Conclusion

The paper verifies the performance of a newly developed adaptive 100% injection-based stator ground fault protection by using fault-free and faulty subharmonic signals acquired from a large MVA generator. This verification was deemed necessary as a prior verification [14] was obtained on a 5 kVA lab generator under some restrictive conditions. In

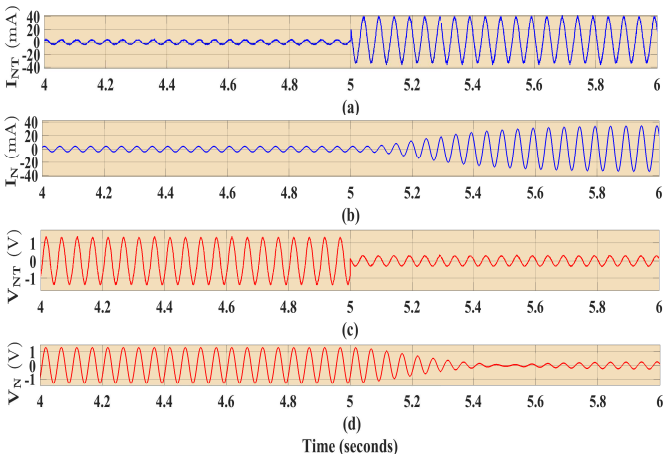

Fig. 15. Case iii) zoomed in signals: (a) Total secondary neutral current I_{NT}, (b) calibrated 20 Hz secondary neutral current I_N, (c) total neutral voltage V_{NT}, and (d) 20 Hz neutral voltage V_N

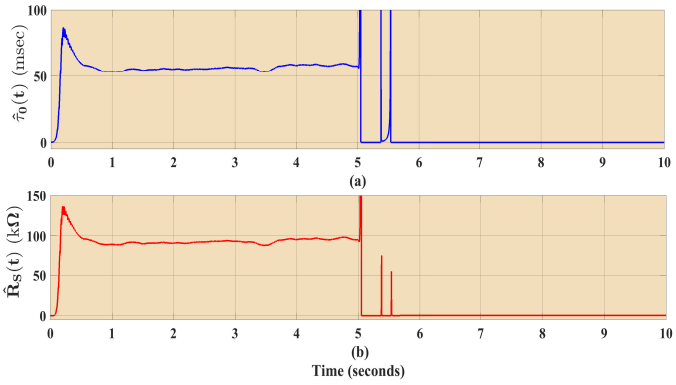

Fig. 16. Case iii): (a) Stator insulation time constant, and (b) stator insulation resistance

particular, small scale of the lab generator resulted in low level subharmonic signals, so additional compensation capacitances had to be added and the use of a normally present CT in the neutral grounding circuit was impractical. In the present paper, neither of these restrictions exist as the new scheme has now been verified using the subharmonic injection signals of a 618 MVA generator with all industrial scale equipment including a CT in the neutral grounding circuit. Although, the presence of this neutral grounding CT necessitated some signal calibration, it must be pointed out that the particular CT used in the 618 MVA generator neutral grounding circuit is a T50 class which is known to have an appreciable core flux leakage effect [23]. While the use of this CT is deemed adequate for application of the conventional overcurrent-based 64S scheme, it is not recommended for the conventional or adaptive impedance-based 64S schemes. For this reason, it is envisioned that the implementation of the new scheme on large generators would use a higher class CT designed for subharmonic applications so that the need for any signal calibrations is entirely eliminated.

ACKNOWLEDGMENT

The authors would like to sincerely thank Professor Giri Venkataramanan of University of Wisconsin-Madison for lending his high precision probes/scope and PhD student Mr. Perry Channegowda who operated them to capture the required signals.

REFERENCES

[1] C. V. Maughan, "Stator winding ground protection failures," presented at the ASME Power Conf., Boston, MA, USA, Jul. 29-Aug. 1, 2013.
[2] D. Reimert, *Protective Relaying For Power Generation Systems,* Boca Raton, FL, USA: CRC, 2006.
[3] IEEE Guide for AC Generator Protection, IEEE Std. C37.102, 2006.
[4] J. W. Pope, "A comparison of 100% stator ground fault protection schemes for generator stator windings," *IEEE Trans. Power App. Syst.*, vol. PAS-103, no. 4, pp. 832840, Apr. 1984.
[5] N. L. Tai, X. G. Yin, Z. Zhang, and D. Chen, "Research of subharmonic injection schemes for hydro-generator stator ground protection," *in Proc. IEEE Power Eng. Soc. Winter Meeting*, 2000, vol. 3, pp. 19281932.
[6] J. Wu, H. Wan, and Y. Lu, "Study of a fresh subharmonic injection scheme based on equilibrium principle for hydro-generator stator ground protection," *in Proc. IEEE Power Eng. Soc. Winter Meeting*, 2002, vol. 2, pp. 924929.
[7] Z. Xiangjun, Y. Xianggen, L. Gan, S. Sheng, and C. Deshu, "Improvement of subharmonic injection schemes for huge hydro-generator stator ground fault protection," *in Proc. Int. Conf. Power Syst. Technol.*, 2002, vol. 2, pp. 707710.
[8] N. Safari-Shad and R. Franklin, "Adaptive 100% stator ground fault protection based on subharmonic injection method," *in Proc. XXIIth Int. Conf. Electr. Mach.*, Lausanne, Switzerland, Sep. 47, 2016, pp. 21512157.
[9] Schneider Electric, MiCOM P345 Generator Protection Relay Technical Manual, 2010.
[10] ABB Inc. Generator Protection REG670 Application Manual, Document ID: 1MRK 502 030-UEN, Rev,. B. Dec. 2012.
[11] Siemens, SIPROTEC 7UM62 V4.6, Multifunction Generator, Motor and Transformer Protection Relay, Manual no. C53000-G1176-C149-7, Release date 03.2010.
[12] GE Digital, GPM field and stator ground fault protection modules, GE publ. code: 1601-0256-Z1 (GEK-113231B), Feb. 2013.
[13] Schweitzer Engineering Lab Inc., SEL-2664S Stator Ground Protection Relay, Instruction Manual, date code 20140507.
[14] N. Safari-Shad, R. Franklin, A. Negahdari, and H. A. Toliyat "Adaptive 100% injection-based generator stator ground fault protection with real-time fault location capability," *IEEE Trans. on Power Delivery,* vol. 33, no. 5, pp 2364-2372, Oct. 2018.
[15] Beckwith Electric, M3425A Generator Protection Relay Instructional Book, Beckwith Electric Inc. Publ.
[16] A. V. Oppenheim and R. W. Schafer, *Discrete-Time Signal Processing,* 3rd ed. Englewood Cliffs, NJ, USA: Prentice-Hall, 2010.
[17] T. Söderström, and P. Stoica, *System Identification* (System Control Engineering Series). Englewood Cliffs, NJ. USA: Prentice-Hall, 1989.
[18] IEEE Recommended Practice for Measurement of Power Factor Tip-Up of Electric Machinery Stator Coil Insulation, (R2006).
[19] S. B. Lee, K. Younsi, and G. B. Kliman "An online technique for monitoring the insulation condition of ac machine stator windings," *IEEE Trans. on Energy Conv.,* Dec. 2005, pp. 737-745.
[20] R. Preston and J. Kandrac, "Report on design, testing and commissioning of 100% stator ground fault protection at Dominion's Bath County pumped-storage station," in *Proc. of Power Systems Conf.*, 2009, pp. 1-13.
[21] P. Soñez, F. Vicentini, V. Skendzic, M. Donolo, S. Patel, Y. Xia and R. C. Scharlach, "Injection-based generator stator ground protection advancements," *Proc. 41st western protective relay conf.*, Oct. 2014.
[22] S. Turner, "Applying 100% stator ground fault protection by low frequency injection for generators," *Proc. IEEE Power Energy Soc. Gen. Meeting*, Jul. 2009, pp. 1-6.
[23] IEEE Guide for the Application of Current Transformers Used for Protective Relaying Purposes, IEEE Std. C37.110, 2007.

VI. BIOGRAPHIES

Nader Safari-Shad was born in Tehran, Iran in 1960. He received the B.S. and M.S. degrees in electrical engineering from Oregon State University in 1982 and 1984. He received the Ph.D. degree in electrical engineering from University of Wisconsin-Madison, in 1992.

From 1992 to 2000, he was with the electrical engineering department at K.N. Toosi University of Technology in Tehran, Iran. Since 2001, he has been with the electrical and computer engineering department at University of Wisconsin-Platteville and has held a consulting position with the System Protection Department at Alliant Energy Corporation. Since September 2014, he has been serving as a member of several subcommittees at the IEEE-PES Power Systems Relaying and Control Committee.

Russ Franklin was born in Cedar Rapids, IA in 1967. He received the B.S. degree in electrical engineering from Iowa State University in 1990.

From 1990 to present, he has worked for 29 years in the utility industry for Alliant Energy Corporation. During this time he has worked in various positions supporting engineering design, construction and operational support of Transmission, Distribution and Generation facilities. Currently, he is a Senior Manager Electrical Engineering. His research interests include power system protection.